Title

Dirt's Hidden Defenders: Antibiotic Production in the Rhizosphere of Sage Hill

Authors

Maldonado, Esteffani
Louie, Madeline
Kho, Kyra
et al.

Publication Date

2024-08-26

Undergraduate

Dirt's Hidden Defenders: Antibiotic Production in the Rhizosphere of Sage Hill

Culture Crew
Kyra Kho (806065350, kkho16@g.ucla.edu)
Madeline Louie (305617171, maddiel@g.ucla.edu)
Esteffani Maldonado (805384843, esteffani101001@g.ucla.edu)
Mordecai Wesenachin (705506562, wesenacm@g.ucla.edu)
MIMG 109AL, Winter Quarter 2024
Dr. Tejas Bouklas
Dominic Garza

Introduction

Antibiotic production in the rhizosphere is an area with potential for novel discovery since studies of this topic are limited due to challenges presented by traditional culture-based techniques (Sait et al., 2002). Knowledge of this activity would be beneficial in a number of areas, including agricultural sustainability and medicine. Recently, outbreaks of plant diseases have risen, reducing crops and endangering global food security (Ristaino et al., 2021), and understanding microbial relationships with plants can help prevent plant diseases and aid in crop production since beneficial bacteria could be utilized to boost plant immune function (Hou et al., 2020). However, this is not possible without first examining antibiotic species in the rhizosphere, as well as their interactions with plants and other rhizobacteria. Furthermore, as antibiotic resistance becomes more widespread, it is becoming increasingly more critical that new antibiotic drugs are discovered to replace medications that are no longer effective against bacterial infections (Walsh et al., 2023). A majority of antibiotics that are distributed today are developed from soil microorganisms (Salam et al., 2023). Thus, understanding the existence and behavior of antibiotic producing bacteria in the rhizosphere can provide insights into finding novel antibiotic compounds.

Similarly, studying interactions between plants and microbes provides promising avenues for new mechanisms of antibiotic action. Symbiotic interactions hold functions that aid in the growth and survival of plants, including immune functions (Hou et al., 2020). In particular, antibiotic production is a mechanism employed by rhizobacteria to combat plant pathogens, assisting in maintaining plant growth (Alori and Babalola, 2018). Plant growth promoting microbes are groups of microorganisms that associate with the roots and promote the growth of plants and protect them from external abiotic stressors and plant pathogens (Dhawi, 2023). For example, microorganisms like *B. substilis* benefit from symbiosis with plants by increasing the

efficiency of antibiotic production to outcompete other microbes for selection by the host plant; in return, *B. substilis* increases the immunity of the plant host to pathogenic plant bacteria (Ogran et al., 2019). In addition, *P. fluorescens* has been shown to grow on plant root surfaces to protect plants from fungal and bacterial phytopathogen; this was demonstrated when a radish with antibiotics from *P. fluorescens* in the water was able to grow more than the control without antibiotics with little to no bacterial growth (Nakata et al., 2014). While studies exist showing that antibiotic producing bacteria form a symbiotic relationship with plants, there is a possibility for the plant pathogens to develop resistance to the antibiotic. Plant pathogens can transmit mobile genetic elements to horizontally transfer antibiotic resistance genes (Chen et al., 2023). As antibiotic resistance increases, plant growth may decrease from being unable to combat the plant pathogen with antibiotics. Antibiotic production and resistance plays a multifaceted role in plant growth, which will be explored further.

Another facet worthy of investigation is the frequency of antibiotic production within the rhizosphere of native plants and non-native plants, which would provide a greater understanding of the ecological impact of invasive species. Native plants tend to have more antibiotic producers in their rhizosphere than non-native plants (Bowens 2017). According to Dr. Andrew Kleinhesselink, managing director of Sage Hill at UCLA within the Institute of Environment and Sustainability, the plants that were found at our soil collection site were likely *Artemisia californica* (California Sagebrush) and *Stipa pulchra* (purple needlegrass), both native plant species to the California coast. *Since* rhizobacteria, which exist in a symbiotic relationship with plants, uphold functions essential to plant survival and influence plant fitness through antibiotic production (Hou et al., 2020), *if* antibiotic producing bacteria are beneficial to plants and exist in a symbiotic relationship, *then* there will be bacteria with antibiotic producing properties in the

rhizospheres of native plants in recently restored environments. Many attributes of soil shape the composition and diversity of the microbial community. Studies have shown that soil pH correlates with microbial diversity and richness, and higher diversity is associated with neutral pH values (Fierer et al., 2006). Diversity levels are measured by the Shannon Index, a summary variable that incorporates phylotype richness and evenness (Fierer et al., 2006). *Since* environmental factors such as pH influence antibiotic microbial diversity by affecting microbial growth and metabolism (Mendes et al, 2013), *if* the soil from Sage Hill demonstrates microbial diversity and thus following this pre-existing inclination, *then* the Shannon Index value of the soil sample would be higher relative to soil with more acidic or basic characteristics.

The overall goal of this project is to bridge the knowledge gap in the types, functions, and roles of antibiotic producing bacteria that exists in plant rhizospheres in recently restored areas like Sage Hill. This project will investigate the antibiotic producing bacteria present in the soil of Sage Hill, the function of these antibiotic producing bacteria in the rhizosphere and how antibiotic producing bacteria impacts plants. Functional assays were performed to assess the presence of antibiotic production, antibiotic resistance, and plant-growth promoting capabilities in the sample; as well as biochemical assays which characterized the bacteria residing in the soil. Not only were antibiotic producing and resistant bacteria identified, but bacteria isolates with antibiotic producing and resistant properties also showed zones of color change on siderophore production or phosphorus solubilization plates, indicating a potential connection between plant growth and antibiotic properties of bacteria. Based on the biochemical assay results, it is possible that the presence of bacteria species such as *Pseudomonas* and *Bacillus* resides within the soil rhizosphere of Sage Hill. These potential discoveries will guide further research into the

characterization of the unknown bacteria within the sample through cultivation-independent approaches such as metagenomics.

Materials/Methods

Soil Collection:

Soil samples were taken from Sage Hill, a recently restored grassland terrestrial habitat located in the Northwest corner of UCLA campus. We recorded the following features concerning the environmental conditions, such as the weather temperature, and humidity levels. We also recorded the soil depth from which samples were taken, along with what plant species they were located near. Soil samples were stored at 4°C for the remainder of the research project.

Soil Characterization (pH, Water Content, Active Carbon, NPK):

A number of tests were done to characterize the collected soil. One of the tests involved soil pH testing. A small soil sample was vortexed with distilled water, then tested using a pH strip. The strip color was compared to a pH reference chart alongside a distilled water control to determine pH values.

Another soil characterization test measured the soil water content. For each of two trials, the mass of sieved soil was recorded in an aluminum weighing dish before drying the soil completely in an oven at 105°C and measuring the soil mass to calculate water content.

Active soil carbon was also measured to further characterize the soil. The soil sample was added to diluted Potassium Permanganate solution and shaken, and the settled liquid was tested for absorbance using a spectrophotometer set at 550 nm.

The nitrogen, phosphorus and potassium levels of the soil sample were measured according to the protocols outlined by the LaMotte NPK Soil Kit (Weil et. al., 2003).

Enrichment and Purification of Isolates

Initial enrichment was performed onto 4 distinct media types: RDM, R2A, ISP4, and N2-BAP. Using aseptic technique, 10^{-2} to 10^{-8} dilutions of soil samples were plated on each

media type, totalling 28 plates. Plates were incubated at 30°C up to one week before selection of isolates. The final isolate count by the end of the quarter was 15, but to ensure that the methodology is recorded with utmost accuracy, all of the procedures will be described with the original isolate quantities tested. All further work done with the isolates was carried out under BSL-2 safety protocol.

Pure cultures were isolated from mixed populations by utilizing the streak plate procedure, and colonies were plated according to the quadrant method. Plates were incubated at 30°C for 24-48 hours for R2A and 48 hours -1 week for ISP4. Weekly streak plating was performed on each isolate to maintain purity and fresh cultures, which were stored in the cold room. The isolated cultures were named using this nomenclature: Quarter/Year/School ID/Lab Section/Team Initials/Growth Condition/Isolate #. For simplicity, isolates will be referred to using just the isolate number and media type (e.g. W24UCLA1091ACC30R15 will be called R15). Isolated colonies were also converted into liquid cultures by inoculating them into a 3-5ml broth of whichever plate media they were grown on.

Gram staining is able to show the purity and cell morphology of bacterial isolates. Gram staining was performed both manually and by machine. Manually, the isolates were smeared on a slide until it was turbid and dried. The left and right droplet contained *M. luteus* (positive control) and *E. coli* (negative control) respectively. Then, methanol fixation occurred. Afterwards, crystal violet stain was added followed by iodine, ethanol, and safranin. Rinsing with distilled water was done after each step of staining and ethanol. The slide was dried and viewed under Kohler illumination microscopy for cell morphology and gram stain color. This process was repeated for all isolates. For the machine, the 9 isolates were smeared in their respective squares on the slide with less tap water used; the slide had a positive control. The

machine completed staining and fixation before Kohler Illumination microscopy. The pure isolates went through functional and biochemical assays for further characterization.

To visualize bacterial motility, wet mounts were prepared using bacterial isolates grown on agar plates. Using an inoculating loop, one colony isolate of bacteria was emulsified in tap water on a clean slide. A coverslip was then gently placed over the slide and a microscope was set to Kohler Illumination. The wet mount was then viewed under phase contrast microscopy. Some of the isolates were viewed under 100X magnification utilizing oil immersion.

Functional Assays

To determine which pure isolates produced antibiotics, functional assays for antibiotic production were carried out. Isolates were plated with a lawn of indicator strain bacteria (*Escherichia coli*, *Kocuria rhizophila*, and mutant *E. coli*) and zones of inhibition were observed. Mutant *E.coli* was plated on LB$_{cam}$ while *E. coli* and *K. rhizophila* were plated on LB plates. Since there were 20 isolates, 10 isolates were put on one antibiotic production plate and 3 plates were used for each control, which resulted in a total of 9 indicator strain plates. These plates were labeled and a grid was drawn where isolates were placed to observe zones of inhibition. A cotton swab was briefly dipped into the control and streaked onto its plate to grow a lawn. This was left to dry and the liquid culture was vortexed. The liquid culture isolate was streaked onto the designated square on the plate. This was repeated for all the isolates on each indicator strain plate. It was incubated at 30°C for 24-48 hours.

To test for antibiotic resistance, liquid cultures were used to grow isolates on Mueller-Hinton agar plates. Mueller-Hinton plates were fully inoculated using a cotton swab to streak the entire surface.After drying for 15 minutes, four different antibiotic discs were placed on the plate. For gram-positive bacteria, the antibiotics tested were tetracycline, kanamycin,

clindamycin, and penicillin. For gram-negative bacteria, the antibiotics tested were tetracycline, ciprofloxacin, streptomycin, and cefuroxime. The control created for each isolate did not use antibiotic discs. These plates were then incubated at 30℃ for 24-48 hours.

To determine siderophore production in the isolates, overnight liquid cultures were prepared of the unknown bacteria, followed by inoculation in groups of three isolates on one CAS plate, along with a positive control of *E. coli*. Plates were incubated at 30℃ for 1-7 days to observe zones of color change.

Phosphate solubilization capability was assessed through the preparation of overnight liquid cultures of the isolates, then inoculation of the cultures onto Pikovskaya Phosphate (PVK) plates in groups of three along with the positive control of *Burkholderia unamae*. The cultures were also spotted onto PVK + bromocresol purple plates along with the same control to assess pH changes through changes in color. All plates were incubated at 30°C for 1-7 days.

Biochemical Assays

For each isolate, the presence of the enzyme catalase was assessed by fixing a small amount of bacteria onto a clean slide and exposing the bacteria to hydrogen peroxide. The absence or presence of bubbles following the addition of hydrogen peroxide was recorded. *E. coli* (catalase positive) and *Enterococcus* (catalase negative) were included as controls when performing the experiment.

To determine the presence of fermentative or oxidative metabolism of carbohydrates in the isolates, the oxidation-fermentation (OF) test was performed. Two OF-glucose deeps were inoculated with one unknown culture along with a positive control (*Pseudomonas stutzeri*) and a negative control (*Alcaligenes faecalis*), with mineral oil being added to one of the deeps to simulate an anaerobic environment. The deeps were incubated at 35 C for 48 hours.

SIM media was used to test for sulfur reduction, indole production, and cellular motility. SIM media was inoculated with either an isolate or one of 3 controls: *E. coli* (indole and motility), *M. luteus* (negative control), and *C. freundii* (sulfur reduction), and was poked straight down on the SIM media until around 1 cm from the bottom to prevent contact. Incubation occurred at 30℃ for 24 hours.

Mannitol Salt Agar plates were used to determine mannitol fermentation and growth under high salt conditions. 6 MSA plates were obtained and four isolates were divided on one plate for a total of 5 MSA plates. Another plate had *S. capitis* (positive control) and *E. coli* (negative control). An isolate was streaked in the shape of a smiley face on the MSA plate. This was repeated for each isolate. It was incubated at 30℃ for 24 hours.

TSIA was used to determine glucose, lactose, and sucrose fermentation along with sulfur reduction. For TSIA experiments, 20 isolates were inoculated into a respective TSIA slants, along with 3 controls: *E. coli* (glucose, lactose, and/or sucrose fermentation), *A. faecalis* (no fermentation), and *C. freundii* (sulfur reduction). An isolate or control was picked and stabbed into the agar until it reached the bottom of the tube. Incubation occurred at 30℃ for 24 hours.

DNA extraction and PCR amplification

To extract genetic material from soil microorganisms, DNA was isolated directly from the sample. Soil microorganisms were lysed utilizing heat, chemical, and mechanical disruption through the Invitrogen PureLink™ Microbiome DNA Purification Kit, the reagents involved being described in more detail through the MIMG 109AL Lab Manual. Inhibitors that may have been present in the sample were removed through proprietary cleanup, and then the sample was placed into a PureLink™ spin column for purification. Lastly, the purified DNA bound to the column underwent a wash step before extraction.

16S rRNA amplification of the isolated colonies was performed if direct isolation of genomic DNA failed. A colony was placed directly into a PCR tube that contained Master Mix composed of the following primers and reagents: PCR Primer 1492R, PCR Primer 27F, 10X PCR Buffer, 25 mM MgCl2, sterile distilled water, and 10 mM dNTPS. 7 portions of Master Mix were made for 19 PCR samples. Master Mix was pipetted into each PCR tube and kept on ice, while 7 LB plates were prepared for colony PCR to show isolate growth. Three PCR samples and 1 negative control were placed on each plate. Isolates were picked on the LB plate followed by insertion into their PCR tubes. LB plates were incubated at 30°C for colony growth. Lastly, the PCR tubes were placed into a 96-well thermocycler and ran in the denaturation, annealing, and extension cycle, beginning with hot-start lysis and DNA denaturation at 98℃, followed by adding TAQ polymerase and restarting the program.

The PCR samples were run on a 0.8% agarose gel composed of TAE buffer and DNA-SAFE stain. The gel was placed into the electrophoresis chamber filled with 1X TAE buffer and PCR samples, prepared with a 1:3 ratio of 6X dye and sample, were loaded alongside a kb ladder in the gel. Electrophoresis ran for 25 minutes at 110 mA, which differed from the lab manual (30 minutes at 95 mA) due to time constraints. When electrophoresis finished, the DNA bands were viewed with a UV gel-imaging system. The image and legend were recorded (Figure 4).

Results

Soil Characterization & Isolate Purification

In order to understand the environmental context of the isolated microbes, several soil characterization tests were performed. Average gravimetric moisture content over two trials was 19.101%; additionally, the pH of the soil was determined to be 6, identical to the distilled water

control. Meanwhile, active carbon testing indicated that the active soil carbon in the soil sample is 632.2 $\frac{mg}{kg}$. Use of the NPK Soil Kit has also allowed for further soil characterization, yielding a result of low amounts of nitrogen and phosphorus and trace amounts of potassium. These soil characterization results provided better context for the strains isolated.

After growing soil bacteria on a variety of media, diverse representations of culturable bacteria were achieved. The colonies that had appeared on the plates demonstrated immense variety in morphology, with representative images of enrichment plates and streak plates being seen in Figure 1. After inspection of growth, ISP4 and R2A were selected as the media types to use in further isolation, as they demonstrated significant growth and ISP4 is selective for the *Streptomyces* species, known for antibiotic production. 28 isolates were initially selected, but over time, isolates were discontinued as different factors rendered them unusable, such as impurities and contamination. From these plates a final total of 15 active isolates were chosen to work with for the remainder of the quarter, whose characteristics are summarized in Figure 2. Moving on to results for bacterial isolates, the first round of streak plating resulted in a mixture of successfully isolated colonies and plates that did not demonstrate any colonies but did demonstrate growth. Many plates that showed a variety of colony colors and morphologies were obtained, providing the basis for the subsequent experiments aimed at observing and characterizing this diversity.

Gram Status, Motility and Morphology for Bacterial Isolates

To better characterize the unknown isolates and determine cellular morphology, gram-staining was utilized. Results for gram-staining indicated a total of 10 gram negative bacteria and 5 gram positive bacteria. Of these, 6 of them resembled a bacillus morphology, 3 resembled a coccus morphology, and 5 of them resemble a filamentous morphology. For the

unknown bacterial isolates, wet mount results have indicated that all six of the bacteria isolates tested were non-motile. Figure 2 demonstrates gram stain status, motility, and cell morphology for each isolate, as well as representative gram stain images. After characterization of these isolates through observation of their cellular morphology and motility had been completed, functional attributes of the unknown microbes had to be tested.

Functional Assays

After experiments were conducted to better characterize the unknown bacteria through their cellular morphology and motility, functional assays such as antibiotic production, antibiotic resistance, phosphate solubilization, and siderophore production were performed to ensure more characterization of the functional attributes. For antibiotic production, overall 27% (4/15) isolates showed antibiotic production. In addition, 30% of the gram negative and 20% of the gram positive bacteria show antibiotic production (Figure 3a and Figure 3c). The zones of clearances that show antibiotic production for 4/15 isolates range from 14.5 mm to 19 mm (Figure 3b and Figure 3d). Because all of the isolates displaying antibiotic production properties showed zones of clearances on *K. rhizophila,* there is a possibility that the antibiotics produced by the isolates target gram positive bacteria since *K. rhizophila* is gram positive (Figure 3e, Figure 3f, and Figure 3g). To be more specific, 3/15 isolates may produce antibiotics that target both gram positive and gram negative bacteria, which would be an broad spectrum antibiotic, since these isolates showed zones of clearances for both *E. coli* (gram negative) and *K. rhizophila* (gram positive) (Figure 3a and Figure 3c). In general, there were less zones of clearances on *E. coli* and mutant *E. coli* meaning that these indicator strains are more resistant to the antibiotics produced by the isolates (Figure 3a and Figure 3c). However, because 2/15 isolates showed zones of clearances on mutant *E.coli*, there is a possibility that they produce

Vancomycin since mutant *E. coli* was designed to be susceptible to Vancomycin (Figure 3a and Figure 3c). Vancomycin is usually not effective against gram negative bacteria like *E. coli* because it targets cell wall synthesis and is effective against gram positive bacteria so this could be an antibiotic that these isolates produce.

Additionally, from the fifteen unknown bacterial isolates tested for antibiotic resistance, the zone of inhibition measurements ranged from 5 mm to 52 mm among all the antibiotics tested. Four out of fifteen of the isolates demonstrated antibiotic resistance. Figure 4 displays full tables with the diameter of clearing measurements for each isolate and antibiotic used as well as relative antibiotic resistance graphs. Images of the results can be found on Google Drive.

Other plant growth promoting properties were also observed aside from antibiotic functions, such as phosphate solubilization and siderophore production. For the phosphate solubilization assays, of the 15 isolates tested, 73% (11/15) demonstrated zones of clearance on the Pikovskaya phosphate (PVK) plates. However, only 5 of those isolates that demonstrated zones of clearance showed zones of color change (indicative of a change in pH) in the PVK + Bromocresol purple plates.

A different plant-growth promoting property observed was siderophore production. Of the 15 active isolates tested, four demonstrated positive results for siderophore production, indicative through zones of color change. Many isolates demonstrated overlap within the functional assay results, being able to perform more than one of these plant growth promoting functions (Figure 5). The isolates that demonstrated antibiotic producing capabilities all showed positive results for at least one other function, explained in more detail in Figure 5.

Biochemical Assays

This series of biochemical assays were performed to differentiate the isolates on the basis of their metabolic diversity. For MSA, 2/15 isolates showed the ability to do mannitol fermentation, 3/15 isolates can grow under high salt concentrations (Figure 6a). R15 is able to do mannitol fermentation, grow under high salt concentrations, produce antibiotics, and be antibiotic resistant (Figure 6c). For TSIA, 20% of the isolates were able to undergo sulfur reduction, do glucose fermentation, or produce acidic byproducts from glucose fermentation (Figure 6a). In particular, I2, which can produce antibiotics and be antibiotic resistant, can also do sulfur reduction, glucose fermentation, and be motile (Figure 6b). Based on the SIM results, 2/15 isolates are motile and 20% of the isolates can reduce sulfur (Figure 6a and figure 6d). Both SIM and TSIA confirm that isolate I2 has sulfur reduction properties. In addition, 87% of the 15 isolates can do oxidation while 80% can do fermentation (Figure 6a). R1, which is antibiotic resistant and can produce antibiotics, can do both fermentation and oxidation (Figure 6a and Figure 6e). From the catalase test, 67% of the isolates showed up positive so they can convert toxic hydrogen peroxide to oxygen and water and are aerobic respirators (Figure 6a). Based on these results, I2 could be *Bacillus* if it tested positive for endospore staining; R1 and R2 could be *Pseudomonas* if it tested positive for the oxidase test. Both *Pseudomonas* and *Bacillus* are both known to have antibiotic producing and resistance capabilities.

DNA and Genomic Isolation

Lastly, preliminary procedures were performed to prepare for the cultivation-independent phase of the research. DNA was extracted to obtain genetic material from the soil microorganisms in the sample. The DNA isolated directly from the soil for a metagenomic approach demonstrated a purified DNA concentration of 589.9 ng/microliter and a purified DNA ratio of 1.27. The purified DNA concentration is the amount of DNA that was extracted, where a

higher value indicates a higher yield of DNA. The purified DNA ratio is the ratio of nucleic acid to contaminants and the ideal ratio is 1.8.

Colony PCR was also utilized to account for isolates that potentially could not undergo genomic isolation through spin-column technology. Of the 21 isolates that had undergone colony PCR and were run through gel electrophoresis, six isolates demonstrated ideal kb size to be submitted for sequencing. These isolates were R3, R7, R13, I3, I11, and I14. Figure 7 shows the gel pictures of the DNA bands. The five successful isolates are located within lanes 6-10 of the gel seen in Figure 7a, however it is important to note that some of the isolates that demonstrated bands have since been discontinued for impurity. It can be seen that the five isolates line up to the approximately 6th band on the gel, which is 1.5kb. Figure 7b demonstrates the other successful isolates not all tested for in Figure 7a.

Figure 1: Enrichment of bacterial isolates from Sage Hill

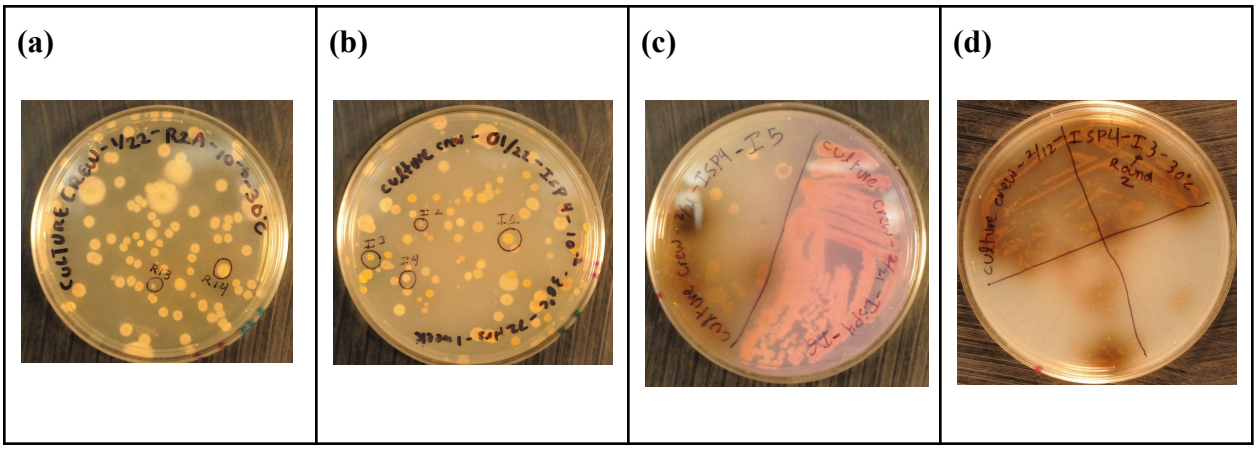

Figure 1. Enrichment of Bacterial Isolates from Sage Hill and Representative Streak Plates. Enrichment plates demonstrate diverse representations of soil bacteria from the dilutions of soil samples onto plates of different media types, such as the selected media like ISP4 and R2A. All plates were incubated at 30℃ for varying periods of time, selective media like ISP4 having longer incubation times than minimal media such as R2A. Figure 1(a) demonstrates initial enrichment onto the R2A plate at 10^{-5} dilution. Figure 1(b) shows ISP4 at 10^{-2} dilution. Colonies selected for further isolation are circled. Representative streak plates are seen for 1(c) and 1(d). In 1(c), the streak plate of Isolates I5 and I6 are shown. These were both plated on ISP4 at 30℃ for 3-5 days. Figure 1(d) is a streak plate of I3 with isolated colonies in quadrants 3 and 4. This isolate demonstrated a black pigmentation. This was plated on ISP4 at 30℃ for 3-5 days.

Isolate Characteristics table

Isolate Name	Macro-morphology	Micro-morphology	Key Functional Assay	Identity Hypothesis
W24UCLA1091ACC30R1	White, circular, surrounded by fuzzy outer circle	Bacillus, G-	Abx production	*Psueodomonas*
W24UCLA1091ACC30R2	clusters on small white circles	G-	Abx production	*Pseudomonas*
W24UCLA1091ACC30R3	small, isolated, white circular colonies	Filamentous, G+	catalase -	
W24UCLA1091ACC30R7	light yellow inner circle with white larger outer ring	Bacillus, G-	Phosphate solubilization +	
W24UCLA1091ACC30R12	dark brown, circular	Filamentous, G-	Sulfur reduction +	
W24UCLA1091ACC30R13	small light brown	Filamentous, G- non-motile	Glucose Fermentation -	
W24UCLA1091ACC30R14	dark brown inner circle, fuzzy yellow ring, white outer layer	Coccus, G- non-motile	Sulfur reduction +	
W24UCLA1091ACC30R15	medium, pink, oval	Coccus, G- non-motile	Abx production	
W24UCLA1091ACC30I2	small yellowish brown	Bacillus, G+	Abx production	*Bacillus*
W24UCLA1091ACC30I3	yellow with brown center	Filamentous, G+ non-motile	Siderophore, phosphate Solubilization +	
W24UCLA1091ACC30I4	white with dark small fuzzy inner circle	Bacillus, G-	Siderophore, phosphate Solubilization +	
W24UCLA1091ACC30I6	brown with fuzzy outer ring	Bacillus, G+ non-motile	Siderophore, phosphate Solubilization +	
W24UCLA1091ACC30I11	medium, circles, yellow	Filamentous, G-	Siderophore, phosphate Solubilization +	
W24UCLA1091ACC30I13	medium, yellow	G-	Phosphate solubilization +	
W24UCLA1091ACC30I14	dark brown, undefined circular shapes.	Coccus, G+ non-motile	Phosphate solubilization +	

Isolate Characteristics Table. Summary chart of the selected isolates for this research project. Isolates were selected as a team effort through observation colony characteristics on the enrichment plates, or plates of different media such as ISP4 and R2A incubated at 30℃ for 48 hours-1 week and 24 hours-48 hours, respectively. The chart demonstrates the proper isolate name, its media type, the colony morphology, the cell morphology, the gram status, the motility, and whether or not the isolate has successfully undergone PCR. The information is available for most isolates, however a few isolates have not been investigated yet for all of the factors within this table due to time constraints.

Figure 2: Gram Status, Motility and Morphology for Bacterial Isolates

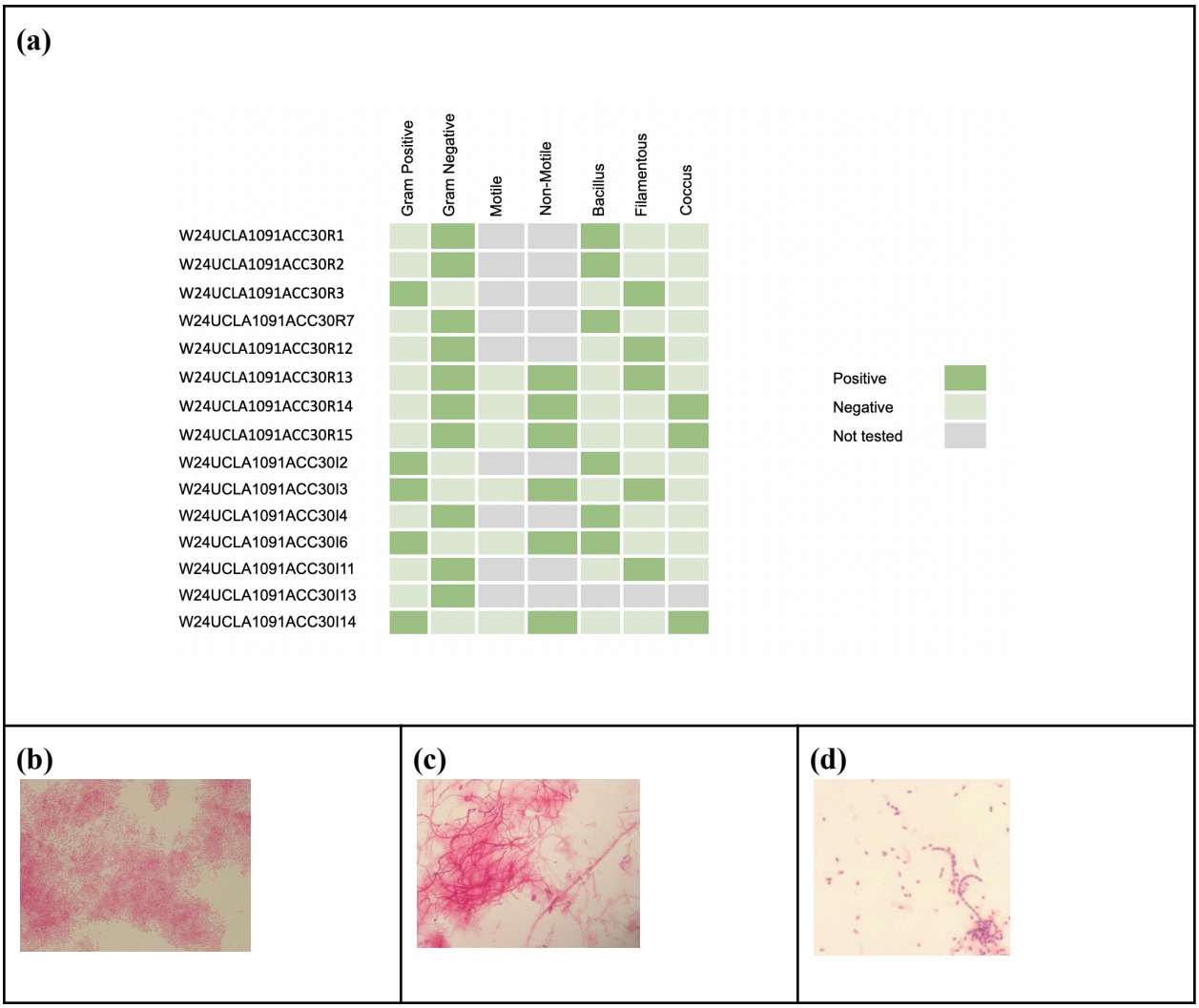

Figure 2. Gram staining and cell morphology. (a) This map depicts the gram status, motility, and cell morphology of each individual isolate as determined by gram staining and wet mounts. Dark green represents positive test results, light green represents negative test results, and gray indicates that the isolate was not tested. **(b)** This image shows a gram negative, bacillus morphology from R1 isolate. **(c)** This image shows a gram negative, filamentous morphology from R12 isolate. **(d)** This image shows a gram positive, coccus morphology from I14 isolate. Positive control was *M. luteus* and negative control was *E. coli*.

Figure 3: Antibiotic Production Assay Results

a) Graph of Approximate Antibiotic Production Assay for Gram Negative Isolates

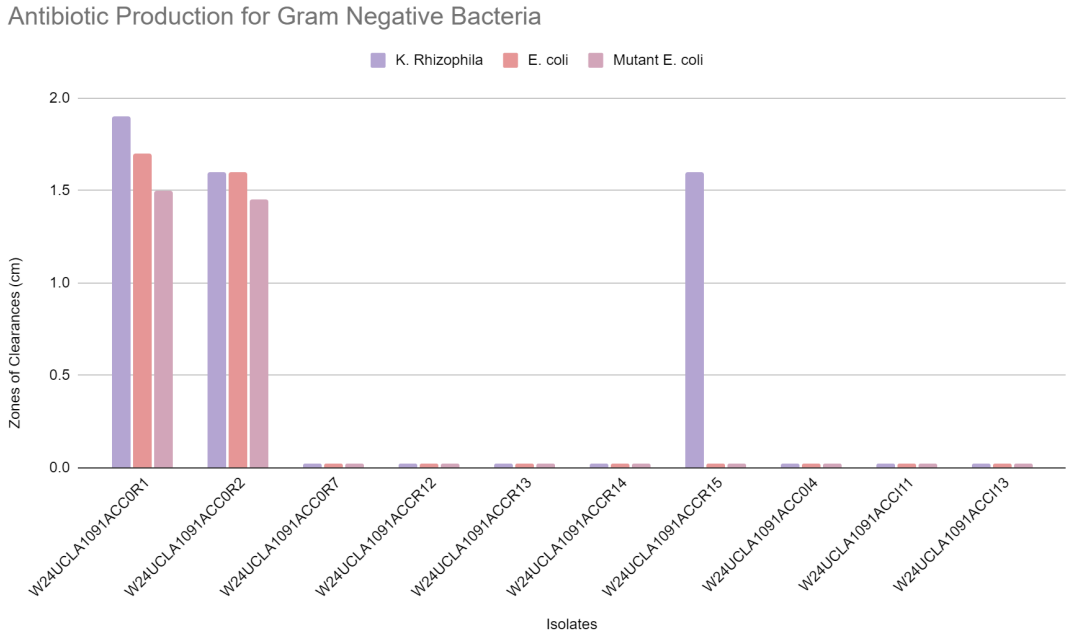

b) Table of Antibiotic Production Assay Results for Gram Negative Isolates

	Zones of clearances (cm)		
	K. Rhizophila	*E. coli*	Mutant *E. coli*
W24UCLA1091ACC0R1	1.9	1.7	1.5
W24UCLA1091ACC0R2	1.6	1.6	1.45
W24UCLA1091ACC0R7	0	0	0
W24UCLA1091ACCR12	0	0	0
W24UCLA1091ACCR13	0	0	0
W24UCLA1091ACCR14	0	0	0
W24UCLA1091ACCR15	1.6	0	0
W24UCLA1091ACC0I4	0	0	0
W24UCLA1091ACCI11	0	0	0
W24UCLA1091ACCI13	0	0	0

c) Graph of Approximate Antibiotic Production Assay for Gram Positive Isolates

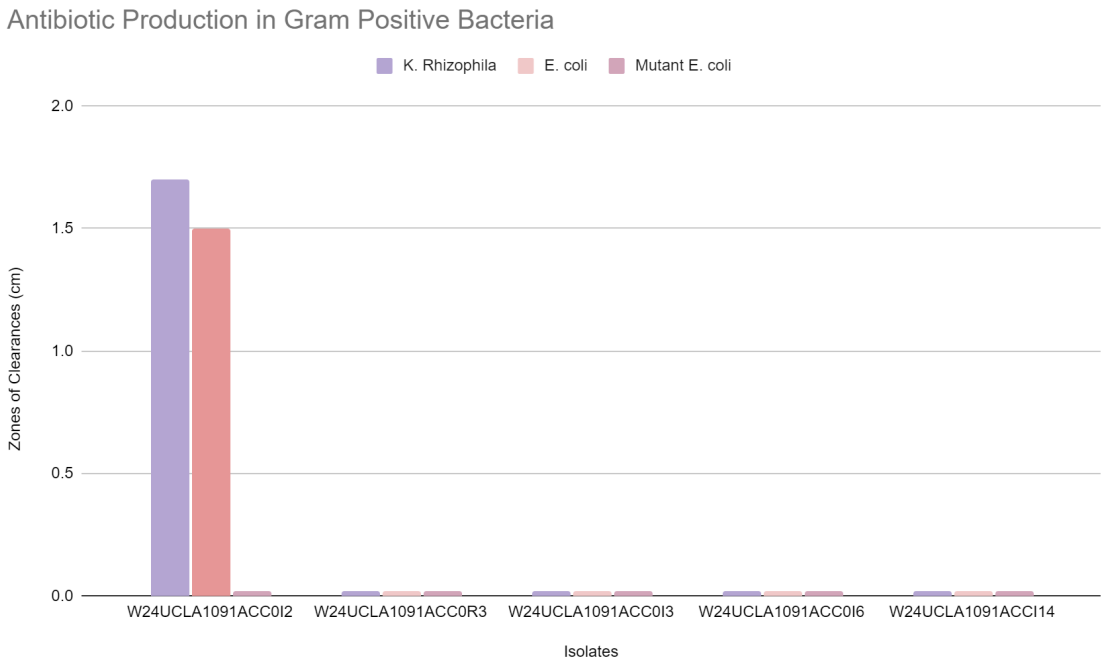

d) Table of Antibiotic Production Assay Results for Gram Negative Isolates

	Zones of Clearance (cm)		
	K. Rhizophila	*E. coli*	Mutant *E. coli*
W24UCLA1091ACC0I2	1.7	1.5	0
W24UCLA1091ACC0R3	0	0	0
W24UCLA1091ACC0I3	0	0	0
W24UCLA1091ACC0I6	0	0	0
W24UCLA1091ACCI14	0	0	0

(e)

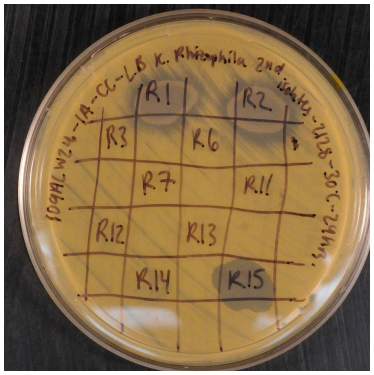

(f)

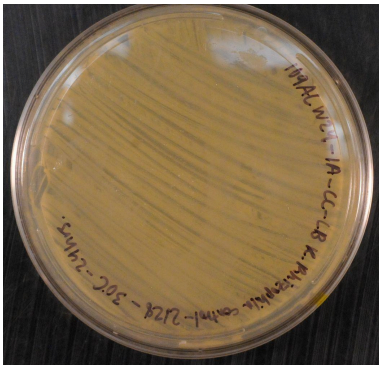

(g)

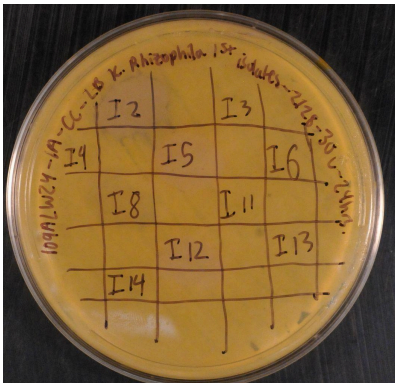

Figure 3. Antibiotic Production Assay Results. (a) This graph shows the distribution of zones of clearances across all the indicator strains (*K. rhizophila, E. coli,* and mutant *E. coli*) for each gram negative isolate that produced antibiotics. **(b)** This table shows the diameter (cm) of each zone of clearances showing antibiotic production for each gram negative isolate across the indicator strains. **(c)** This graph shows the distribution of zones of clearances across all the indicator strains for each gram positive isolate that produced antibiotics. **(d)** This table shows the diameter (cm) of each zone of clearances showing antibiotic production for each gram positive isolate across the indicator strains. **(e)** This plate shows the zones of clearances on *K. rhizophila* and it is visible on isolates R1, R2, and R15. **(f)** This is the control and *K. rhizophila* was able to create a lawn. **(g)** This plate shows the zones of clearances on *K. rhizophila* and it is visible on isolate I2. *K. rhizophila* plates were incubated at 30℃ for 24 - 48 hours.

Figure 4: Antibiotic Resistance Assay Results

a) Table of Antibiotic Resistance Assay Results for Gram Positive Isolates

Gram Positive Isolates	Tetracycline	Clindamycin	Kanamycin	Penicillin
W24UCLA1091ACC30R3	20 mm	21 mm	52 mm	5 mm
W24UCLA1091ACC30I2	24 mm	23 mm	28 mm	5 mm
W24UCLA1091ACC30I3	17 mm	14 mm	38 mm	27 mm
W24UCLA1091ACC30I6	22 mm	12 mm	52 mm	20 mm
W24UCLA1091ACC30I14	9 mm	14 mm	38 mm	27 mm

b) Table of Antibiotic Resistance Assay Results for Gram Negative Isolates

Gram Negative Isolates	Tetracycline	Cefuroxime	Streptomycin	Ciprofloxacin
W24UCLA1091ACC30R1	18.5 mm	5 mm	12 mm	31 mm
W24UCLA1091ACC30R2	17 mm	5 mm	11 mm	38 mm
W24UCLA1091ACC30R7	Complete	Complete	Complete	Complete

	Susceptibility	Susceptibility	Susceptibility	Susceptibility
W24UCLA1091ACC30R12	17 mm	15 mm	36 mm	15 mm
W24UCLA1091ACC30R13	Complete Susceptibility	Complete Susceptibility	Complete Susceptibility	Complete Susceptibility
W24UCLA1091ACC30R14	19 mm	29 mm	43 mm	27 mm
W24UCLA1091ACC30R15	29 mm	7 mm	18 mm	31 mm
W24UCLA1091ACC30I4	21 mm	Complete Susceptibility	40 mm	22 mm
W24UCLA1091ACC30I11	Complete Susceptibility	Complete Susceptibility	Complete Susceptibility	Complete Susceptibility
W24UCLA1091ACC30I13	18 mm	38 mm	32 mm	17 mm

c) Graph of Relative Antibiotic Resistance for Each Gram Positive Isolate

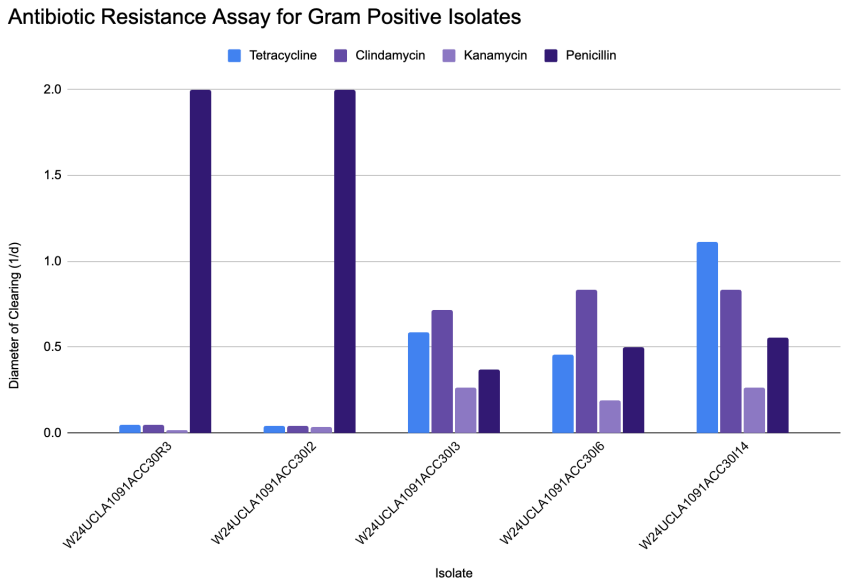

d) Graph of Relative Antibiotic Resistance for Each Gram Negative Isolate

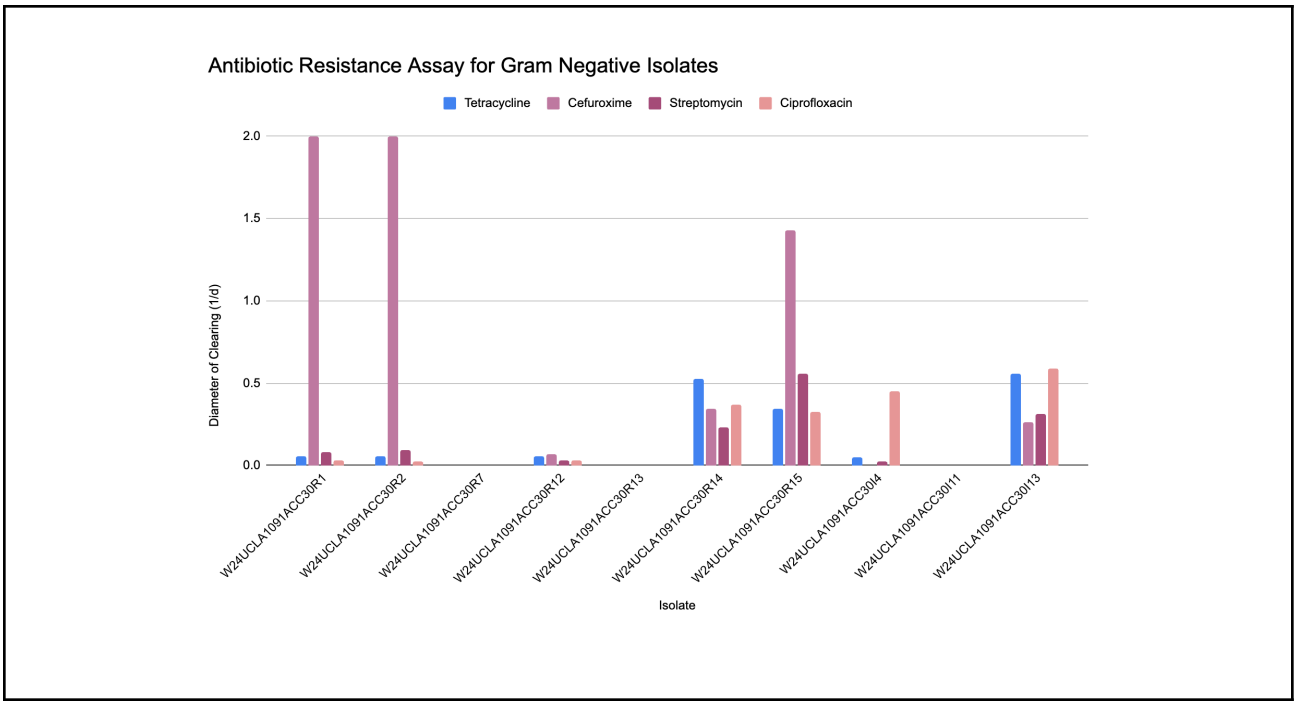

Figure 4. Antibiotic Resistance Assay Results. (a) Table of antibiotic resistance assay results for gram positive isolates. Five isolates were tested against tetracycline, clindamycin, kanamycin, and penicillin and resulting diameters of clearing were measured in millimeters. Mueller-Hinton agar plates were used and incubated at 30°C for 24-48 hours. **(b)** Table of antibiotic resistance assay results for gram negative isolates. Ten isolates were tested against tetracycline, cefuroxime, streptomycin and ciprofloxacin and resulting zones of inhibition were measured in millimeters. Mueller-Hinton agar plates were used and incubated at 30°C for 24-48 hours. **(c)** graph of relative antibiotic resistance for each gram positive isolate using the inverse of the diameter of clearing . **(d)** graph of relative antibiotic resistance for each gram negative isolate using the inverse of the diameter of clearing.

Figure 5: Functional Assay Venn Diagram

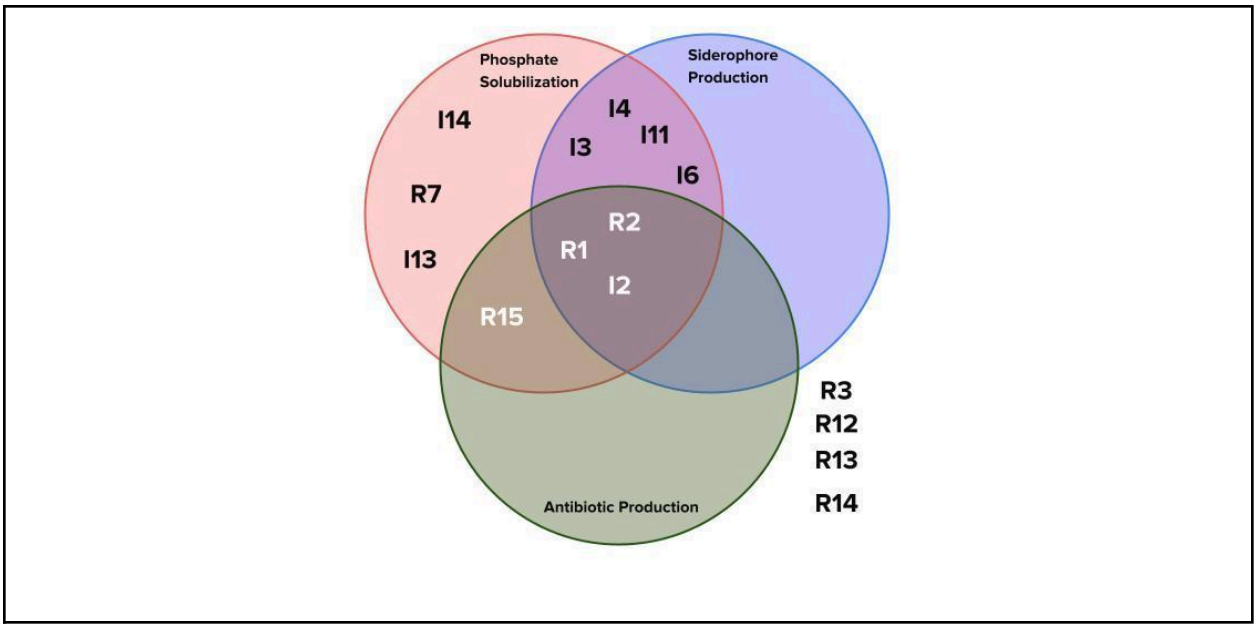

Figure 5. Functional Assay Venn Diagram. Figure 5 shows a Venn diagram demonstrating the isolates that showed positive results in the following functional assays; phosphate solubilization, siderophore production, and antibiotic production. Isolates were compared against a positive control of *B. unamae* for phosphate solubilization, a positive control of *E. coli* for siderophore production, and a negative control for antibiotic production in which bacterial lawns of the following indicator strains were prepared with no inoculation of the unknown bacteria: *K. rhizophila*, wt *E. coli*, and (mutant) *smpA surA E. coli.* The Venn diagram demonstrates only the isolates that are still currently active. Of the fifteen tested, eleven showed positive results for any of the three functional assays. One isolate, R15, showed antibiotic producing capabilities as well as phosphate solubilization capabilities. Three isolates, R2, R1, and I2, demonstrated positive results for all three capabilities. The isolates left out of the venn diagram to the right did not show zones of clearances or color change in any of the assays involved.

Figure 6: Biochemical Assay Results

(a)

(b)

(c)

(d)

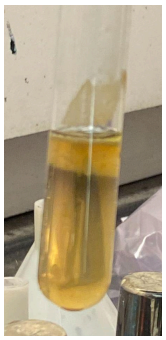

(e)

Figure 6. Summary of Biochemical Assay Results. (a) A map of the pure isolate results for the biochemical assays. Positive results were indicated in dark green while red showed a negative result, and gray represented the isolates that did not do the biochemical test. The isolates put in red text on the far left column are the isolates that showed antibiotic production and resistance. **(b)** I2 isolate shows sulfur reduction and glucose fermentation with an accumulation of acid production through TSIA. **(c)** R15 shows mannitol fermentation and grows under high salt concentrations through MSA. **(d)** I2 shows sulfur reduction through SIM. **(e)** R1 shows oxidation and fermentation through oxidation fermentation test. All of the biochemical assays were incubated at 30℃ for 24 - 48 hours. *E. coli* (catalase positive) and *Enterococcus* (catalase negative) are controls. Positive control (*Pseudomonas stutzeri*) and a negative control (*Alcaligenes faecalis*) are controls for oxidation-fermentation test. The controls for SIM are: *E. coli* (indole and motility), *M. luteus* (negative control), and *C. freundii* (sulfur reduction). The controls for MSA are: *S. capitis* (positive control) and *E. coli* (negative control). The controls for TSIA are: *E. coli* (glucose, lactose, and/or sucrose fermentation), *A. faecalis* (no fermentation), and *C. freundii* (sulfur reduction).

Figure 7: Colony PCR Gel electrophoresis results

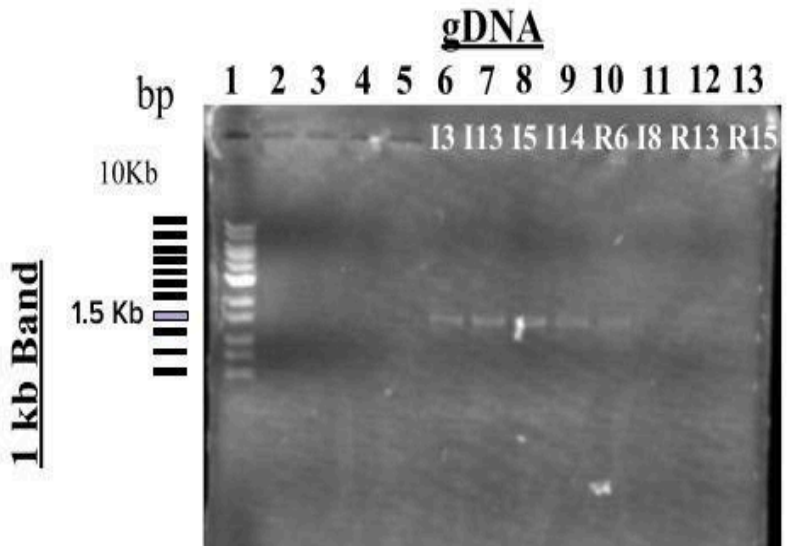
gDNA
bp
1 2 3 4 5 6 7 8 9 10 11 12 13
I3 I13 I5 I14 R6 I8 R13 R15
10Kb
1.5 Kb
1 kb Band

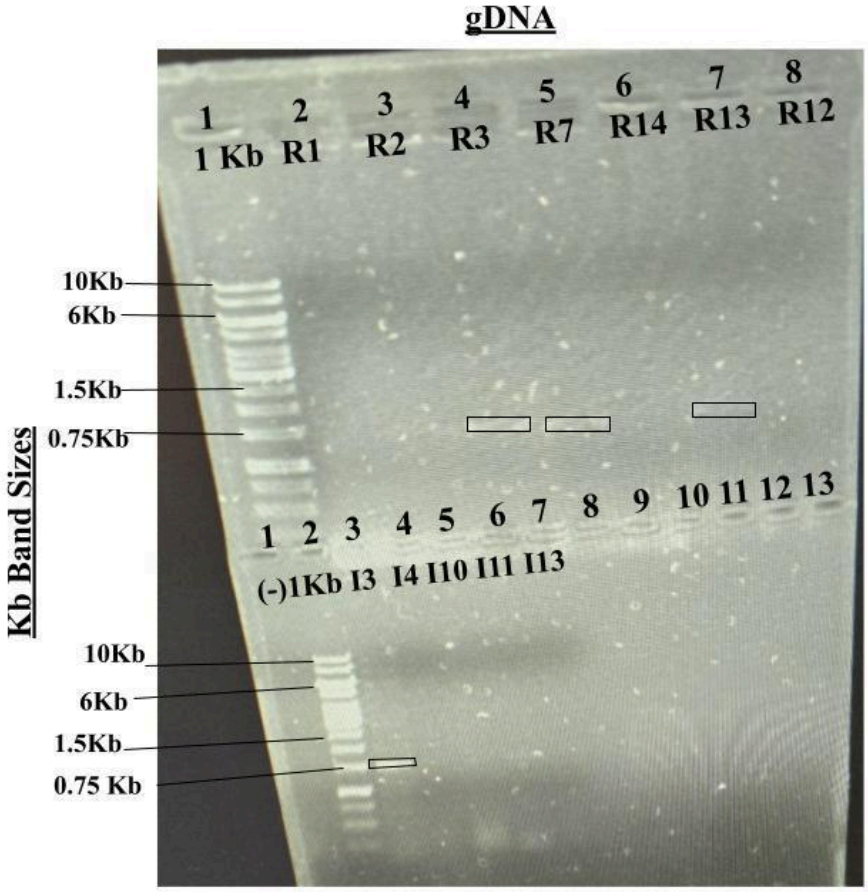
gDNA
1 2 3 4 5 6 7 8
1 Kb R1 R2 R3 R7 R14 R13 R12
10Kb
6Kb
1.5Kb
0.75Kb
1 2 3 4 5 6 7 8 9 10 11 12 13
(-)1Kb I3 I4 I10 I11 I13
Kb Band Sizes
10Kb
6Kb
1.5Kb
0.75 Kb

Figure 7. Gel Electrophoresis pictures. Both panels demonstrate a 0.8% agarose gel composed of agarose, TAE buffer, and DNA Safe-Stain. Each gel was placed within an electrophoresis chamber and electrophoresed for 25 minutes at 110 mA. **(a)** Lanes 6-10 demonstrate successful PCR products (amplicons) of the corresponding isolates; I3, I5, I14, R6, and I8. The current DNA band sizes are presented on the image, with the successful isolates lining up at the band that is 1.5 Kb. **(b)** Higher UV light is utilized to highlight the bands that are not as easy to visualize. In the top panel, successful bands are seen for isolates R3, R7, and R13. In the bottom portion, I3 is seen as a successful band, alongside the 1 Kb ladder that acts as a positive control and the negative control, which is just a sample of Master Mix. Successful isolates demonstrated a band at 0.75 kb.

Discussion

Several key results of soil characterization are worth discussing. Neutral soil pH values are correlated with rhizosphere diversity. First, the pH of the soil measured to be within a neutral range has a relationship with biodiversity in the soil rhizosphere. Previous study has concluded that a neutral pH is correlated with increased microbial diversity, which indicates a relatively wide range of bacterial diversity compared to more acidic or alkaline soil samples (Fierer et al, 2006).Variation in the gram status and cell morphology of purified isolates has indicated a diverse range of bacteria found within the rhizosphere at Sage Hill. Additionally, the isolates demonstrated variation in macro-morphology regarding shape and color. The range in morphologies, as described by Table 1, supports the correlation between neutral pH and microbial diversity. It is also suspected that the black isolates seen on I3 and I11 (in the Google Drive) are likely sulfate reducing bacteria (Uniyal et al., 2002).

Regarding other soil characterization results, nutrient level testing revealed trace amounts of nitrogen, potassium, and phosphorus. According to a prior study, increased NPK levels promote soil microbial growth and diversity, so this nutrient scarcity can indicate a harsher environment, leading to greater competition for limited resources. In addition, since there will be greater competition for the limited resources, it can be hypothesized that the greater inter-microbial competition increases the adaptive advantage of soil-microbe symbiosis, since rhizobacteria can influence plant fitness through antibiotic production (Hou et al., 2020).

Previous studies have also indicated a relationship between native plants and antibiotic producing bacteria, and that native plants have a higher proportion of antimicrobial biosynthesis pathways compared to invasive plants (Bowens et al., 2017). This relationship between native plants and antibiotic producing bacteria is suspected to be the result of rhizosphere microbial

community composition being dictated by plant lineage (Bowens et al., 2017). Having found four isolates that produce antibiotics, out of fifteen, their presence corroborates that antibiotic producing bacteria exist in the rhizospheres surrounding native plants. Additionally, these findings support the hypothesis that antibiotic producing bacteria would be identified in the rhizosphere of native plants in recently restored environments.

For the antibiotic producing bacteria, antibiotic production provides the adaptive advantage of inhibiting the growth of competing bacteria; in addition, these antibiotic producers need to harbor antibiotic resistance mechanisms to protect themselves from their own antibiotics to prevent self-toxicity, which is likely where antibiotic resistance genes have originated from (Kobayashi et al., 2007). This connection suggests that antibiotic resistance may hint at the type of antibiotic produced by the isolates which do antibiotic production. Since isolates R1 and R2 produced antibiotics and indicated resistance to cefuroxime, it is possible they produce antibiotics belonging to the cephalosporin family. Moreover, antibiotic producing isolate I2 indicated resistance to penicillin indicating that I2 may produce antibiotics belonging to the penicillin category. It is important to note that this is not conclusive and more testing needs to be done to confirm these speculations.

Moreover, while investigating antibiotic production as a mechanism for plant fitness and growth was the primary focus of this research, isolated bacteria from the soil demonstrated other plant growth promoting functions as well. All antibiotic producing isolates also indicated phosphate-solubilization capabilities. Since low phosphorus levels were observed in the soil sample, a connection can be made between the soil phosphorus deficiency and the proliferation of phosphate-solubilizing bacteria, as studies have shown that these bacteria convert insoluble phosphorus forms in soil to soluble phosphorus that plants and microbes alike can readily uptake

(Pan and Cai, 2023). Increasing phosphorus access through phosphate solubilization is another function for plant growth promotion aside from antibiotic production, and likely occurs in the sampled environment.

Similar to phosphate solubilization, bacteria that colonize the rhizosphere and perform siderophore production promote the uptake of iron (Fe) by plants through this mechanism, increasing and regulating the availability of this metal (Timofeeva et al., 2022). Siderophore production within the rhizosphere of the soil was seen in similar quantities to the antibiotic production results. However, connections made from these observations are very limited as the levels of iron in the soil sample were not observed.

These conclusions have shed some insights on the research goals, but it is imperative to acknowledge constraints. Cultivation bias refers to the inability to culture most microorganisms under traditional laboratory conditions, leading to an unrepresentative view in terms of phylogeny and diversity (Ling et al., 2015). As a result, investigation into antibiotic production in the rhizosphere was limited to culturable microbes that may misrepresent the greater microbial community in the rhizosphere at Sage Hill. In addition, attempts to perform genomic analysis on isolates necessitates PCR, which creates biases including overrepresentation of lineages with greater numbers of RNA operons. To address this, several factors can mitigate the effect of cultivation bias in cultivation-dependent work, such as using polymeric growth substrates and longer incubation periods, and cultivation-independent procedures, such as bioinformatic tools and community-level analyses. Also, the trial counts for functional assays testing the cultivation-dependent hypothesis were statistically insignificant since one trial of antibiotic production and antibiotic resistance assays were utilized for data analysis. This leads to data variability and limited precision. Lastly, the uncertainty of working with unknown isolated

bacteria creates limitations in experimental design. Unknown bacteria may have unique growth requirements, which were unaccounted for and affect the overall growth of the bacteria limiting the reliability and representative power of this research. However, these findings can still be applied to larger implications. More insight was found on antibiotic production from a novel source, the Sage Hill rhizosphere, and characterization of the soil bacteria will be beneficial for maintenance and care for one of the most ecologically diverse areas of UCLA. Furthermore, this new knowledge about antibiotic development at Sage Hill highlights the need for further research to be conducted not just within the UCLA confines, but into agricultural ecosystems to better understand plant-microbial relationships and refine crop practices. The discovery of antibiotic producing bacteria also provides encouragement to continue the search for new antibiotic development amidst escalating resistance. The findings of this research have assisted in providing a preliminary framework for further efforts in comprehending the relationship between antibiotic-producing rhizobacteria and their broader ecosystem.

Future Directions

To address cultivation bias, cultivation-independent approaches can be employed to study both phylotype diversity and metabolic function, allowing for a more complete functional analysis than observations from soil sample extraction and isolation (Gill et al., 2006). Afterwards, computational genome assembly can be done through a reference genome database or *de novo* assembly. From the extracted genomic data, annotation can be performed and bioinformatic tools like COG and KEGG can reveal metabolic functions. With these tools, the presence and mechanism of antibiotic production can study sequences that better represent the rhizosphere of the soil sample.

Strong correlations between plant composition and the soil microbiome influence have yet to be established (Leff et al., 2018). It is beneficial to observe how plant attributes explain soil microbial diversity through cultivation independent methods such as gene and illumina sequencing, and plant phylogeny (Leff, et al., 2018). An alternate approach observes the effects of co-evolutionary dynamics on the plant-microbe community. Plant species influence the selection of rhizosphere microbiota through factors like plant community productivity and eukaryotic interactions, leading to potential host-microbiome coevolution, which could lead to phylogenetic relatedness (Fields & Friman, 2022).

The Shannon diversity index is a metric quantifying the diversity of soil microbiome for the cultivation independent hypothesis. After submitting the successful PCR samples for sequencing, quantifying, and calculating the taxa and its abundance in the sample, the Shannon diversity index can be determined. Higher values of the Shannon index indicate greater microbial diversity, which is hypothesized from a neutral range soil pH. Observing the sequencing data from peers can develop a more complete profile on the diversity of Sage Hill.

Author Contributions

Everyone practiced restreaking each isolate so there would be a fresh batch for each test done. Madeline and Mordecai collected the soil sample from Sage Hill while Esteffani and Kyra recorded the surrounding environment including taking pictures of the soil sample site at Sage hill. For soil characteristics, Mordecai and Esteffani measured the pH of the soil. Active carbon was done by Mordecai and Kyra. Measuring NPK was done by Mordecai and Esteffani. Water content was done by Mordecai and Kyra. Gram staining for each isolate was done by everyone. Wet mount motility was done by Kyra. For functional assays, liquid cultures for bacterial isolates and controls were done by Madeline. Antibiotic production was done by Kyra. Antibiotic resistance was done by Madeline and Mordecai. Both siderophore production and phosphate solubilization assays were done by Esteffani. For biochemical assays, oxidation-fermentation was done by Esteffani. The Catalase test was done by Esteffani and Mordecai. TSIA, SIM, and MSA were done by Kyra. Colony PCR of isolates was done by Esteffani and Madeline. Everyone ran gel electrophoresis on the colony PCR of each isolate.

References

Borowik, A., & Wyszkowska, J. (2016). Soil moisture as a factor affecting the microbiological and biochemical activity of soil. *Plant, Soil and Environment*, *62*(6), 250-255. doi: 10.17221/158/2016-PSE

Bowen, J. L., Kearns, P. J., Byrnes, J. E. K., Wigginton, S., Allen, W. J., Greenwood, M., Tran, K., Yu, J., Cronin, J. T., & Meyerson, L. A. (2017). Lineage overwhelms environmental conditions in determining rhizosphere bacterial community structure in a cosmopolitan invasive plant. *Nature communications*, *8*(1), 433. https://doi.org/10.1038/s41467-017-00626

Breijyeh, Z., Jubeh, B., & Karaman, R. (2020). Resistance of gram-negative bacteria to current antibacterial agents and approaches to resolve it. Molecules, 25(6), 1340. https://doi.org/10.3390/molecules25061340

Castellano-Hinojosa, A., Strauss, S.L. Insights into the taxonomic and functional characterization of agricultural crop core rhizobiomes and their potential microbial drivers. *Sci Rep* 11, 10068 (2021). https://doi.org/10.1038/s41598-021-89569-7

Chen, P., Yu, K., He, Y. (2023). The dynamics and transmission of antibiotic resistance associated with plant microbiomes, *Environment International,* 176, https://doi.org/10.1016/j.envint.2023.107986.

Dhawi F. (2023). The Role of Plant Growth-Promoting Microorganisms (PGPMs) and Their Feasibility in Hydroponics and Vertical Farming. *Metabolites*, *13*(2), 247. https://doi.org/10.3390/metabo13020247

Fierer, N., & Jackson, R. B. (2006). The diversity and biogeography of soil bacterial communities. *Proceedings of the National Academy of Sciences of the United States of*

America, *103*(3), 626–631. https://doi.org/10.1073/pnas.0507535103

Fields, B., Friman, V.P. (2022). Microbial eco-evolutionary dynamics in the plant rhizosphere, *Current Opinion in Microbiology.* 68, 1369-5274. https://doi.org/10.1016/j.mib.2022.102153.

Gill, S. R., Pop, M., Deboy, R. T., Eckburg, P. B., Turnbaugh, P. J., Samuel, B. S., Gordon, J. I., Relman, D. A., Fraser-Liggett, C. M., & Nelson, K. E. (2006). Metagenomic analysis of the human distal gut microbiome. *Science (New York, N.Y.)*, *312*(5778), 1355–1359. https://doi.org/10.1126/science.1124234

Hou, Q., & Kolodkin-Gal, I. (2020). Harvesting the complex pathways of antibiotic production and resistance of soil bacilli for optimizing plant microbiome. *FEMS microbiology ecology*, *96*(9), fiaa142. https://doi.org/10.1093/femsec/fiaa142

Kobayashi, T., Nonaka, L., Maruyama, F., & Suzuki, S. (2007). Molecular evidence for the ancient origin of the ribosomal protection protein that mediates tetracycline resistance in bacteria. *Journal of molecular evolution*, *65*(3), 228–235. https://doi.org/10.1007/s00239-007-9006-z

Leff, J.W., Bardgett, R.D., Wilkinson, A., Jackson, B.G., Pritchard, W.J., De Long, J.R., Oakley, S., Mason, K.E., Ostle, N.J., Johnson, D, Baggs, E.M., Fierer, N., (2018). Predicting the structure of soil communities from plant community taxonomy, phylogeny, and traits, *The ISME Journal*, Volume 12, Issue 7, July 2018, 1794–1805, https://academic.oup.com/ismej/article-lookup/doi/10.1038/s41396-018-0089-x

Ling, N., Wang, T. & Kuzyakov, Y. Rhizosphere bacteriome structure and functions. *Nat Commun* 13, 836 (2022). https://doi.org/10.1038/s41467-022-28448-9

Mendes, R., Garbeva, P., & Raaijmakers, J. M. (2013). The rhizosphere microbiome:

significance of plant beneficial, plant pathogenic, and human pathogenic microorganisms. *FEMS microbiology reviews*, *37*(5), 634–663. https://doi.org/10.1111/1574-6976.12028

Mohanram, S., Kumar, P. (2019). Rhizosphere microbiome: revisiting the synergy of plant-microbe interactions. *Annals of Microbiology,* 307-320.

Nakata, K., Harada, N., Sumitomo, K., & Yoneda, K. (2000b). Enhancement of plant stem growth by flocculation of the antibiotic-producing bacterium, Pseudomonas fluorescens S272, on the roots. *Bioscience, Biotechnology, and Biochemistry*, *64*(3), 459–465. https://doi.org/10.1271/bbb.64.459

Ogran, A., Yardeni, E. H., Keren-Paz, A., Bucher, T., Jain, R., Gilhar, O., & Kolodkin-Gal, I. (2019). The Plant Host Induces Antibiotic Production To Select the Most-Beneficial Colonizers. *Applied and environmental microbiology*, *85*(13), e00512-19. https://doi.org/10.1128/AEM.00512-19

Singh, P., Chauhan, P. K., Upadhyay, S. K., Singh, R. K., Dwivedi, P., Wang, J., Jain, D., & Jiang, M. (2022). Mechanistic Insights and Potential Use of Siderophores Producing Microbes in Rhizosphere for Mitigation of Stress in Plants Grown in Degraded Land. Frontiers in microbiology, 13, 898979. https://doi.org/10.3389/fmicb.2022.898979

Ristaino, J. B., Anderson, P. K., Bebber, D. P., Brauman, K. A., Cunniffe, N. J., Fedoroff, N. V., Finegold, C., Garrett, K. A., Gilligan, C. A., Jones, C. M., Martin, M. D., MacDonald, G. K., Neenan, P., Records, A., Schmale, D. G., Tateosian, L., & Wei, Q. (2021). The persistent threat of emerging plant disease pandemics to global food security. *Proceedings of the National Academy of Sciences of the United States of America*, *118*(23), e2022239118. https://doi.org/10.1073/pnas.2022239118

Sait, M., Hugenholtz, P., & Janssen, P. H. (2002). Cultivation of globally distributed soil bacteria

from phylogenetic lineages previously only detected in cultivation-independent surveys. *Environmental microbiology*, *4*(11), 654–666. https://doi.org/10.1046/j.1462-2920.2002.00352.x

Salam, M. A., Al-Amin, M. Y., Salam, M. T., Pawar, J. S., Akhter, N., Rabaan, A. A., & Alqumber, M. A. A. (2023). Antimicrobial Resistance: A Growing Serious Threat for Global Public Health. *Healthcare (Basel, Switzerland)*, *11*(13), 1946. https://doi.org/10.3390/healthcare11131946

Shrestha, B., Nath, D. K., Maharjan, A., Poudel, A., Pradhan, R. N., & Aryal, S. (2021). Isolation and Characterization of Potential Antibiotic-Producing Actinomycetes from Water and Soil Sediments of Different Regions of Nepal. International Journal of Microbiology, 2021, e5586165. https://doi.org/10.1155/2021/5586165

Timofeeva, A. M., Galyamova, M. R., & Sedykh, S. E. (2022). Bacterial Siderophores: Classification, Biosynthesis, Perspectives of Use in Agriculture. *Plants (Basel, Switzerland)*, *11*(22), 3065. https://doi.org/10.3390/plants11223065

Uniyal, Sandeep & Chaudary, Lal & Kala, Anju & Agarwal, Neeta. (2022). Isolation and characterization of sulphate reducing bacteria from goat rumen and its inclusion to improve in vitro feed fermentation. The Indian Journal of Animal Sciences. 92. 96-100. 10.56093/ijans.v92i1.120932.

Walsh, T.R., Gales, A.C., Laxminarayan, R., & Dodd, P.C. (2023). Antimicrobial Resistance: Addressing a Global Threat to Humanity. *PLoS medicine*, *20*(7), e1004264. https://doi.org/10.1371/journal.pmed.1004264

Yang, Zhi-Jian, Xiao-Hui Wu, Lan-Ming Huang, Wei-Wei Xie, Yu Chen, Yousry A. El-Kassaby, and Jin-Ling Feng. (2021). "Soil Bacteria to Regulate *Phoebe bournei* Seedling Growth

and Sustainable Soil Utilization under NPK Fertilization" *Plants* 10, no. 9: 1868. https://doi.org/10.3390/plants10091868